SCIENCE CHINA
Technological Sciences

August 2012 Vol.55 No.8: 1–9
doi: 10.1007/s11431-012-4949-8

Preform-based toughening technology for RTMable high-temperature aerospace composites

YI XiaoSu*, CHENG QunFeng & LIU ZhiZhen

Beijing Institute of Aeronautical Materials, Beijing 100095, China

Received May 7, 2012; accepted May 23, 2012

This article describes the efforts that led to the development of surface-loaded preforms that may be used to significantly improve the compression-after-impact strength of high-temperature composites and correspondingly to dramatically reduce the area of damage because of impact. Moreover, by matching the toughening polymer surface-loaded and design of the surface pattern, in-plane mechanical properties are unaffected or even improved over laminates made from the identical materials. The proprietary preforms, so-called ES™-Fabrics, may be handled and infused with the high-temperature RTMable resins such as bismaleimide and polyimide in exactly the same manner as traditional fabrics without surface modification. The RTM conditions for the preform-based toughening is fully compatible with the traditional process procedure, making the technology cost-effective in production. This technology represents a key enabler for the use of low-cost RTM processes for high-temperature resins to supplant prepreg as the building-block material of choice for aeronautical composite structures.

impact damage, surface loading, preform-based toughening, bismaleimide, polyimide, fracture toughness

Citation: Yi X S, Cheng Q F, Liu Z Z. Preform-based toughening technology for RTMable high-temperature aerospace composites. Sci China Tech Sci, 2012, 55: 1–9, doi: 10.1007/s11431-012-4949-8

1 Introduction

A key to implementing materials on airframes is the ability to improve the impact-damage resistance of the materials. This is particularly critical for high-speed military aircraft where high-temperature resistant composite materials are requested. As well-known these materials are usually low impact-damage resistant.

The current state-of-the-art composite materials used in aircraft production are principally prepreg-based. However, the maturation of composite materials, and particularly their manufacturing methods, will potentially rely on liquid-molding approaches, e.g., resin transfer molding (RTM). To have such processes supplant prepreg-based manufacturing approaches, liquid-molded composites need to have mechanical properties that meet those available from prepregs [1]. Because the fibers used in liquid molding are the same as those used in prepregs, mechanical-property improvements must depend on improved matrix resins and preforms. Obviously, it is more difficult and challenging for the RTMable high-temperature matrix resins, because their molecular structure is intrinsically stiff and thus brittle than that of the intermediate-temperature resins like epoxies.

A few years ago, an innovative concept, so-called *Ex-situ* concept was proposed to improve the impact-damage properties of thermoset resin matrix carbon composites by an interlayer-localized toughening approach [2–5]. "*Ex-situ*" means in the context that instead of using a thermoplastic toughened thermosetting matrix as an entity for the composite, the toughening polymer is first abstracted from the blend and used to surface-load the neat thermosetting resin prepreg. As the prepreg is cured, highly toughened thermo-

*Corresponding author (email: xiaosu.yi@biam.ac.cn)

plastic-rich layers are established spatially in the thin interlayer regions whereas the carbon plies remain still thermosetting resin-rich. The microstructure of the interlaminar layers is characterized by the reaction-induced spinodal phase separated and inverted microstructure. The *Ex-situ* concept has successfully been demonstrated for improvement in impact damage resistance for a number of prepreg-grade composites [6]. The *Ex-situ* toughening technique developed by this concept has been patented, e.g., refs. [7, 8].

Recently, an extensive research program is being conducted at Beijing Institute of Aeronautical Materials to focus on preforms and, specifically, preform-based toughening approaches resulting from the *Ex-situ* concept, with the an emphasis on compatibility with liquid molding of aerospace-grade high-performance matrix resins. Most promising results originated from the program have been published in a Chinese monograph [6]. The present work summarizes partially the results on the preform-based toughening of composites made of high-temperature RTMable matrix resins such as bismaleimide (BMI) and polyimide (PI) to meet property targets based on currently available advanced aeronautical prepreg systems.

2 Experiments

2.1 Polymer materials

A bismaleimide (BMI) under a trade-name of 6421 commercialized by the Beijing Institute of Aeronautics Materials (BIAM) was used as one of the RTMable high-temperature resins in the study. The thermoplastic toughening polymer for the BMI was an amorphous polyetherketone (PAEK) with a functional group of phenolphthalein, with an intrinsic viscosity of 0.30 dl/g and a glass transition temperature (T_g) of 230˚C. The PAEK was supplied by Xuzhou Engineering Plastics Factory, China. The molecular structure of the PAEK is shown in Figure 1.

A thermosetting polyimide (PI)-based RTMable resin denoted as 9731 was also used. The resin indicates a higher temperature resistance than the 6421 BMI and was developed by cooperation between BIAM and Changchun Institute of Applied Chemistry of Chinese Academy of Sciences. Its molecular structure is shown in Figure 2. The temperature-time-transformation (TTT) diagram is also established

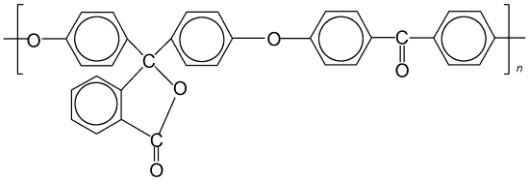

Figure 1 Molecular structure of the PAEK used in the study.

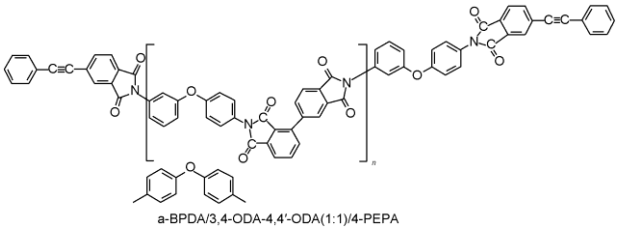

Figure 2 Molecular structure of RTMable polyimide resin (9731).

for process design and manufacturing with the polymer (Figure 3).

The toughening polymer for 9731 resin was a thermoplastic polyimide provided by Jilin University, denoted as 9731T. Its molecular structure (Figure 4) is fully compatible with the thermoset 9731. 9731T exhibits a glass transition temperature higher than 330˚C and its 5% thermal degradation temperature of about 537˚C is very close to that of 9731 at 539˚C tested in air by TG.

2.2 Fiber-reinforcing fabrics and preforms materials

The key component material in the study was the proprietary carbon fiber reinforcing preform commercialized as ES™-Fabrics [7–9].

For liquid-molding it was determined that the use of a highly porous fiber-reinforcing fabric would be desirable. In the patent literature [1], Toray (EP 1 125 728) uses a nonwoven material that comprises both low- (5%–50%) and

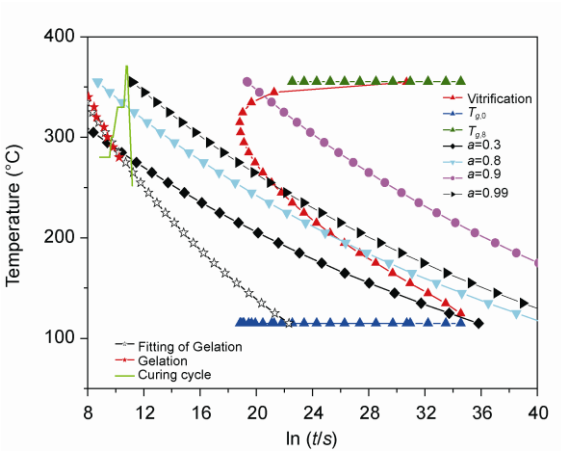

Figure 3 The temperature-time-transformation diagram for 9731 PI.

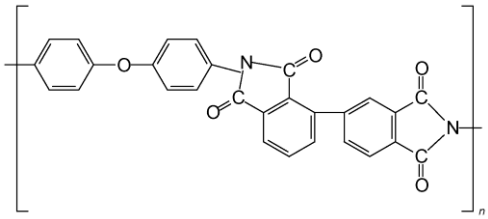

Figure 4 Molecular structure of thermoplastic polyimide (9731T).

high-melt polyamides such that the fabric is attached to the reinforcing material by melt-bonding the low-melt material. Toray further indicates that low-melt materials do not give adequate performance and that crystalline polyamides are preferred because they allow greater toughness improvements at lower loadings. Toray also states that a nonwoven fabric strongly bonded by a thermoplastic polymer is undesirable because the fiber positions are fixed to lose the freedom of deformation. It is obvious that the polyamide can not be used to toughen high-temperature matrices such as BMIs and PIs.

In the study, a commercial G827 carbon cloth (T300-3 k, 160 g±7 g/m^2, Hexcel) as the basic reinforcing fabric was sophisticatedly surface-loaded with various contents of either PAEK or 9731T, as high-temperature toughening polymer by using a special fabrication procedure patented [8]. The trial product is now trade marking registered (ES™-Fabrics). A unique characteristic of the fabrics is the surface pattern (Figure 5) of the toughening polymers, which guarantees the toughness improvement and the permeability of liquid resin in the injection stage. Moreover, one kind of the ES™-Fabrics available is surface-loaded with low-melting binder for performing application, and another one of them available is so-called bi-functional, i.e., surface-loaded with both the binder and toughening agents.

2.3 Specimens preparation

RTM technique was adopted to manufacture the entire composite panel with ES™-Fabrics in close mold. The surface loading level was calculated by wt% in matrix resin for the fabrics. The composite panels were controlled in the thickness of about 3.0–0.1 mm. The overall fiber volume fraction of the panels was controlled at 55% (±2%).

For 6421 BMI [10], the resin was injected at 120˚C under a pressure of 0.2 MPa into the mould in order to impregnate the porous ES™-Fabrics. The mold temperature was raised at a rate of 2°C/min to the two-step curing temperature, followed by a post-curing. After that, the mold was cooled down to 60°C and the composite panel was released. All the RTM panels were finally ultrasonically C-scanned to check for molding defects and to examine the quality according to the aerospace standard specifications. This procedure was applied to all the experiments. Similarly, Figure 6 shows the curing process program for 9731 PI [11].

For comparison, the control systems for both the BMI and PI composites were manufactured in parallel. The basic lay-up of the carbon fabrics and the injection and curing conditions were identical with the control systems using the commercial standard fabrics G827.

2.4 The quasi-static mechanical properties test

The size of the tensile specimen was 230 mm×15 mm according to GB/T3554-1999. The size of the compression specimen was 140 mm×6 mm according to GB/T3856-2005. The size of the flexure specimen was 75 mm×12.5 mm according to GB/T3356-2005. The size of the interlaminar shear strength specimen was 20 mm×6 mm according to GB/T3357-2005. Each mechanical datum reported was an average of five effective tests.

2.5 Compression after impact test

The impact damage resistance of the specimens was characterized by compression after impact (CAI) according to the Boeing commercial airplane group method BSS 7260. The size of the specimens was 150 mm×100 mm×4 mm quasi-isotropic rectangular laminates with plies of $[45/0/-45/90]_{3S}$ using the low-velocity impact energy of 4.45 J/mm.

After the impact, the damage area was evaluated by ultrasonic C-scan. Then the specimens were compressed to obtain the residual compression strength. Each CAI datum reported was an average of three effective tests.

2.6 Fracture measurements

A standard double-cantilever beam (DCB) specimen was

Figure 5 Proprietary ES™-Fabrics and the surface-loading pattern.

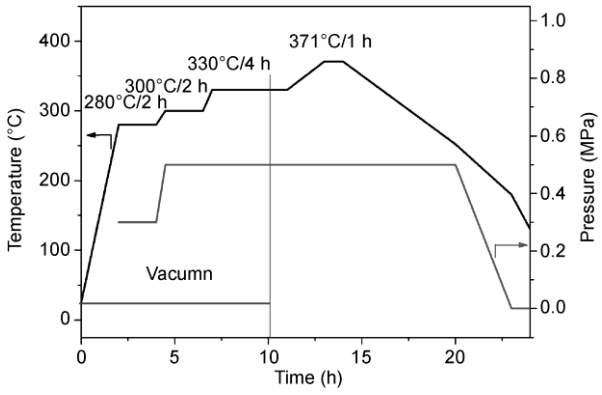

Figure 6 RTM injection and curing process 9731 PI composite specimens.

used to measure Mode I interlaminar fracture toughness according to Chinese Aviation Industry Standard HB 7042-96. A load was applied in the perpendicular direction to the upper surface of the sample at a speed of 2 mm/min. The critical strain energy release rate, G_{IC}, was then calculated.

An end notch flexure (ENF) test specimen was used to measure Mode II interlaminar fracture toughness according to the Chinese Aviation Industry Standard HB 7043-96. The three-point bending apparatus with two stationary support posts of 100 mm apart was used to create shear fracture in the mid-plane. The loading point was in the center between the two stationary posts and the crack tip was at 25 mm from the stationary post. A displacement rate of 2 mm/min was used to load the specimen in flexure until the load decreased upon crack propagation. The Mode II fracture toughness, G_{IIC}, was also calculated at the end of the testing.

2.7 Fractographic studies and cross section observation

The fracture surface of specimens after CAI, Mode I and Mode II tests was observed using a scanning electron microscope (SEM, Hitachi S-3000N). The crack propagation tip was observed using an optical microscope (OM, LEICA DMRME). The specimens were washed in an ultrasonic bath and dried for 4 h at 60°C under vacuum. All specimens for SEM were coated with a gold layer of about 200 Å thick.

3 Results and discussion

All specimens were cut from the RTM panels using ES™-Fabrics as reinforcement material. The investigation was carried out with two PAEK surface-loading levels for 6421 BMI composites and one constant level of 9731T for 9731 PI composites, respectively.

3.1 Compression strength after impact properties

As checked by ultrasonic C-scan after 6421 BMI composite specimen was manufactured, the specimens showed a good quality as-produced by the RTM. By comparing the CAI strength and the delamination area between the control and toughened specimens, Table 1 shows an increase in CAI strength from 155 MPa on the control to 254 MPa of the toughened one with a surface-loading level of 16.8 wt% PAEK. This is an improvement of approximately 65%. The highest increase of about 80% in CAI (277 MPa) is achieved at a PAEK loading level of 20.2 wt%. Correspondingly, the damage area is found to decrease from 1436 to 519 mm^2.

The compression strength properties were also investigated on 9731 PI composites. As shown in Table 2, untoughened specimens were impact-delaminated with an average area of about 715 mm^2, resulting in CAI strength of 137 MPa, whereas the damage area and the residual strength are significantly improved for the 9731T toughened specimens. In the figure, index (F) stands for transfer printing of the 9731T film on the fabric and (P) stands for direct surface loading of the powders [11]. For the both cases, the surface loading level of about 15 wt% 9731T was constant; different were only the application method, surface pattern and the specimen's quality affected by the surface loading methods. As seen, the surface-loading with 9731T film shows slightly a lower delamination area and a higher CAI strength than those with the powder. Obviously, all the test data for 6421 BMI and 9731 PI composites demonstrate a high efficiency of the preform-based toughening concept in improving the impact damage resistance of the high-temperature carbon composites.

Table 1 CAI strengths, impact-damage areas and ultrasonic C-scan results of 6421 BMI composite specimens in dependence on the surface-loading levels of PAEK

Surface-loading level (wt%)	CAI (MPa) /C_v (%)	Damage area (mm^2)	Ultrasonic C-scan
0.0	155/ 2.42	1436	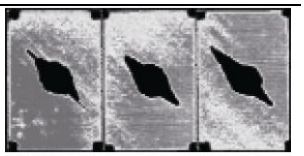
16.8	254/ 3.34	527	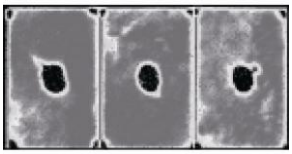
20.2	277/ 2.93	519	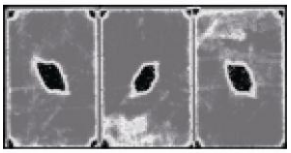

Table 2 CAI strengths, impact-damage areas and ultrasonic C-scan results of 9731 PI composite specimens in dependence on the surface-loading methods of 9731T

Surface-loading level (wt%)	CAI (MPa)	Damage area (mm^2)
0	137	715
15 (P)	249	498
15 (F)	251	475

3.2 Cross section observation of the CAI specimens

A representative impacted specimen from 6421 BMI composites was cut along the long axis in the center and polished to investigate the damage characteristic. Table 3(a) shows the cross-section of the impacted control untoughened. The back surface (bottom in the figure) shows a larger delaminated area with fibers fracture than that of the

Table 3 Representative cross-section photomicroscopes of 6421 BMI composite specimens in dependence on the surface-loading conditions

Control (Untoughened)	
(a) After impact	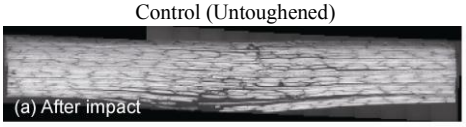
(b) Compression tested after impact	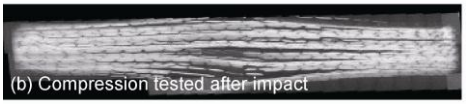
Surface-loaded with 16.8wt% PAEK	
(c) After impact	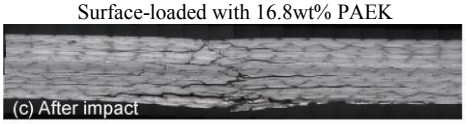
(d) Compression tested after impact	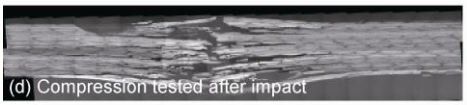
Surface loaded with 20.2wt% PAEK	
(e) After impact	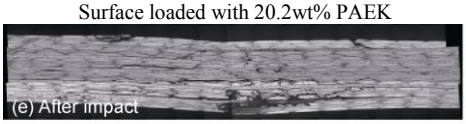
(f) Compression tested after impact	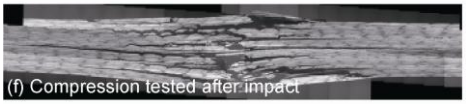

impacted top surface. There were many transverse cracks in the failure area and considerable delamination propagation in the interlaminar regions. Table 3(b) shows the cross-section of the control after CAI test. The failure mode was mainly delamination accompanied with little fiber fracture.

The cross-sections of the composites toughened with two loading levels of PAEK shown in Tables 3(c), (d), (e) and (f), respectively. Both the size of damage cone and the amounts of delamination were found to decrease with an increase in PAEK content. The cross-section of specimens after CAI test revealed that the key energy absorption mechanism was changed from delamination to fiber fracture compared to the control.

Three representative photomicrographs of 6421 BMI composites are shown and compared in Figure 7. It is clear to see that there is a characteristic nodular structure in the interlaminar region for PAEK toughened specimens whereas the untoughened control exhibits a typical brittle fracture. As studied intensively [6], this microstructure is caused by the reaction-induced phase separation and inversion [12]. The BMI particles phase separated and inverted with a diameter of about 0.8 μm are embedded as a dispersed phase in the continuous PAEK phase (Figures 7(b) and (c)). With the PAEK loading level increasing to 20.2 wt%, the size of BMI-rich particles decreases from 0.8 to 0.4 μm. In both cases, the BMI particles were densely interconnected with each other to form a co-continuous microstructure. It should

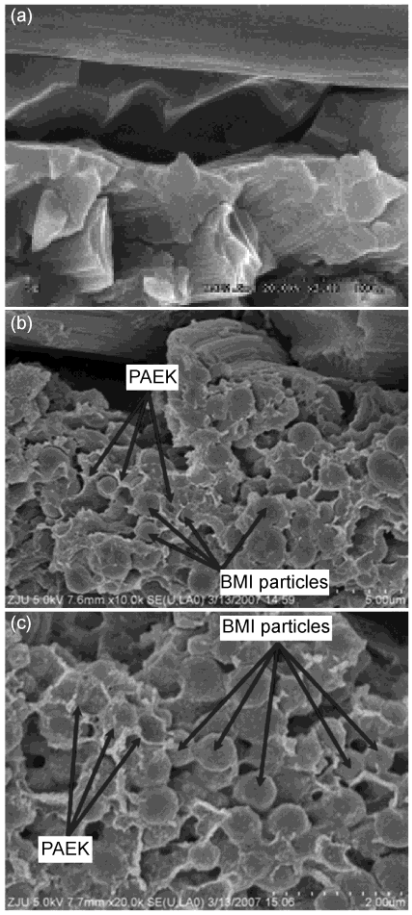

Figure 7 SEM images of interlaminar section of 6421 BMI specimens where PAEK phase was chemically etched in part. (a) Control, untoughened; (b) surface-loading with 16.8 wt% PAEK; (c) surface-loading with 20.2 wt% PAEK.

be noted that the crack propagation caused by out-of-plane impact can be efficiently deflected or bifurcated by the thermosetting particles or stopped by tearing of the thermoplastic phase.

A similar and much finer microstructure was also identified on the 9731 PI composites. The results will be shown in the following section.

3.3 Quasi-static mechanical properties

The test results on 6421 BMI composite preform-based toughened are listed in Table 4. Most of the mechanical properties of composites such as tensile strength, tensile modulus, flexural strength, flexural modulus, and interlaminar shear strength increase a little even when the overall fiber volume fraction decreases slightly because of the limited increase in thickness of composites.

Similarly, 9731 PI composites show promising results even at 288°C (Table 5). Only the interlaminar strength is seen to be decreased at the high temperature.

Table 4 Quasi-static mechanical properties of 6421 BMI composite specimens in dependence on the surface-loading conditions

Mechanical properties	Surface-loading level with PAEK		
	0.0	16.8 wt%	20.2 wt%
0° Tension strength (MPa)	1392	1500	1550
0° Tension modulus (GPa)	102	105	112
Poisson ratio	0.32	0.30	0.34
0° Compression strength (MPa)	1135	1117	1071
0° Compression modulus (GPa)	101	104	110
0° Flexural strength (MPa)	1684	1806	1749
0° Flexural modulus (GPa)	108	115	113
Interlaminar shear strength (MPa)	103	108	104

Table 5 Quasi-static mechanical properties of 9731 PI composite specimens in dependence on the surface-loading and test temperature conditions

		Control	Surface-loaded with 15 wt% 9731T	
			Powder（P）	Film(F)
0° Tension strength (MPa)	25°C	1541	1359	1323
	288°C	1443	1408	1312
0° Tension modulus (GPa)	25°C	113	107	101
	288°C	106	102	103
0° Compression strength (MPa)	25°C	958		
	288°C	827		
0° Compression modulus (GPa)	25°C	113		
	288°C	113		
0° Flexural strength (MPa)	25°C	1726	1639	1467
	288°C	1128	1063	1112
0° Flexural modulus (GPa)	25°C	119	112	96
	288°C	113	113	95.5
Interlaminar shear strength (MPa)	25°C	97.9	108	110
	288°C	56.5	49.3	52.7

3.4 Fracture toughness properties and surface characteristics

Under Mode I test conditions, the load-displacement curves of the 6421 BMI composites are shown in Figure 8, where each triangle represents one loading/unloading cycle. For the control (untoughened), both the initial load and the

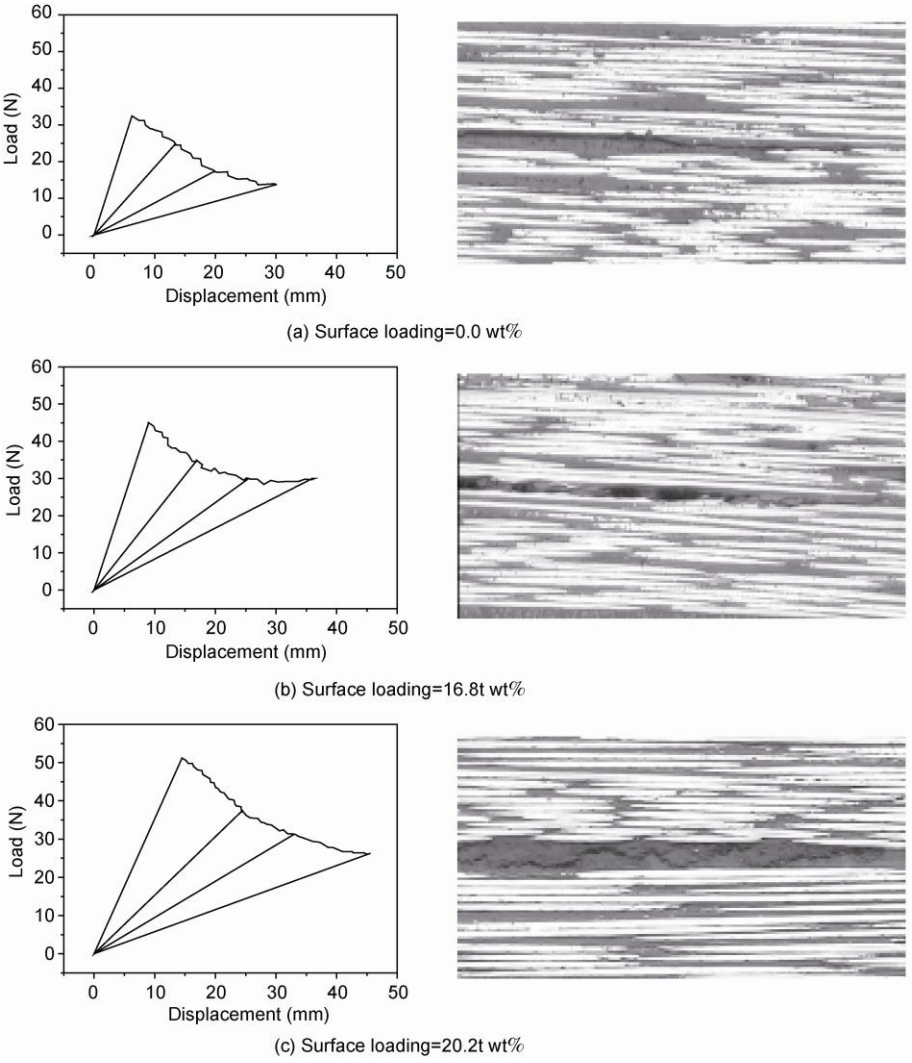

Figure 8 Typical load-displacement curves of the 6421 BMI specimens under Mode I test, and optical images of the crack-tips, where the crack propagates from left to right, in dependence on the surface-loading levels.

ultimate displacement are low, which indicates that the crack, once initiated, propagates quickly, whereas the preform-toughened composites behave against the crack opening and propagation. In addition, the improved resistance is proportional to the surface-loading level.

The crack-tip trace for the 6421 BMI specimens is also shown in the figure in dependence on the toughening conditions. As the optical microcopies exhibit, there is no crack bifurcation or deflection in control. The crack propagates along the interface between the fiber and the matrix, and ends in the BMI-rich region. However, for the toughened composites, the crack deflection, bifurcation, and blunting occurred.

The fracture surfaces were observed by SEM (Figure 9). The characteristic hackle marks are found on the fracture surfaces of all specimens, which are typical under the G_{IC} test conditions leading to shear delamination. The matrix resin fails in a series of parallel cracks which are at an angle of about 45° to the fibers. There is no fiber pullout on the fracture surface, implying that there is no fiber bridging.

On the fracture surface of composites preform-based toughened with 16.8 wt% PAEK, the typical co-continuous microstructure was confirmed. To further explore the toughening mechanism, the onset of crack propagation was carefully investigated. The BMI-rich particles with a small diameter of about 0.8 μm are surrounded by continuous PAEK-rich phase. It was much surprising that the brittle BMI-rich particles were plastically deformed from a shape of globular to elliptical with an angle of about 45° to the fibers (Figure 9). The cavitation or debonding of the particles phases and the plastic yielding of the BMI-rich or PEAK-rich phases are clearly recognized.

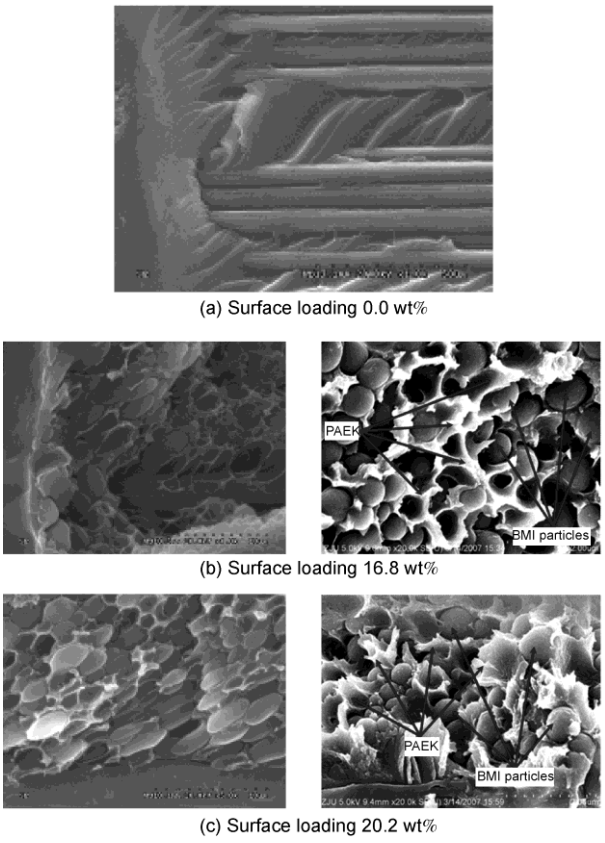

Figure 9 Representative SEM images of fracture surface of 6421 BMI specimens under Mode I test in dependence on the surface-loading levels; the crack propagates from left to right.

As the PAEK loading increases to 20.2 wt%, the diameter of BMI-rich particles decreases to about 0.4 μm. The decrease in particle size is in a good agreement with the reaction-induced phase separation and coarsening mechanism [12]. The cracks propagate through fracture of the continuous PAEK-rich phase by tearing under the local tensile loading conditions. The fracture microstructure looks similar to that of specimens toughened with 16.8% PAEK.

Figure 10 shows and compares the load-displacement curves for 6421 BMI composites untoughened and toughened under Mode II test. As expected, the G_{IIC} performance was enhanced in terms of the shear loading and deformation, for both surface-loading levels, respectively.

The fracture surface of specimens were studied by SEM (Figure 11). At high magnification, the PAEK-rich phase appears to be sheared or torn under Mode II condition instead of cavitation or debonding.

To have an overview, the G_{IC}, G_{IIC} and the coefficient of variation (C_v) are listed in Table 6. The G_{IC} of 215 J/m^2 and G_{IIC} of 510 J/m^2 for the neat BMI composites are typical for the brittle matrix composites reinforced with the high volume fraction of carbon fibers. However, both values rise twice higher than that of the control after that the composites are preform-toughened with 20.2 wt% PAEK.

9731 PI composite specimens were also tested in G_{IC} and G_{IIC} (Figures 12 and 13). For a constant surface-loading level of about 15 wt% 9731T, by using film (F) or powder (P), the improvements of G_{IC} and G_{IIC} toughness were obviously significant (Table 7).

Unlike the microstructure observed on the fracture surface of 6421 BMI composite under G_{IC} and G_{IIC} conditions, a much finer nodular microstructure was found to be chara-

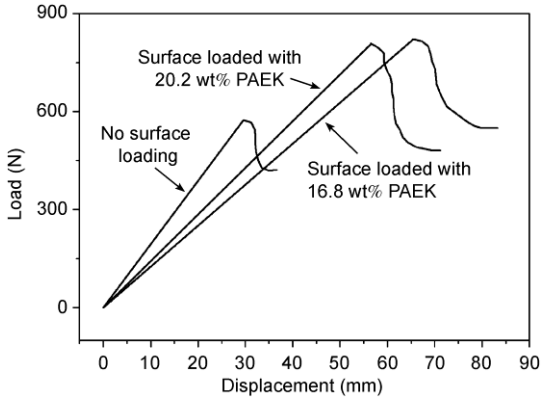

Figure 10 The load-displacement curves of the 6421 BMI specimens in dependence on the surface-loading conditions.

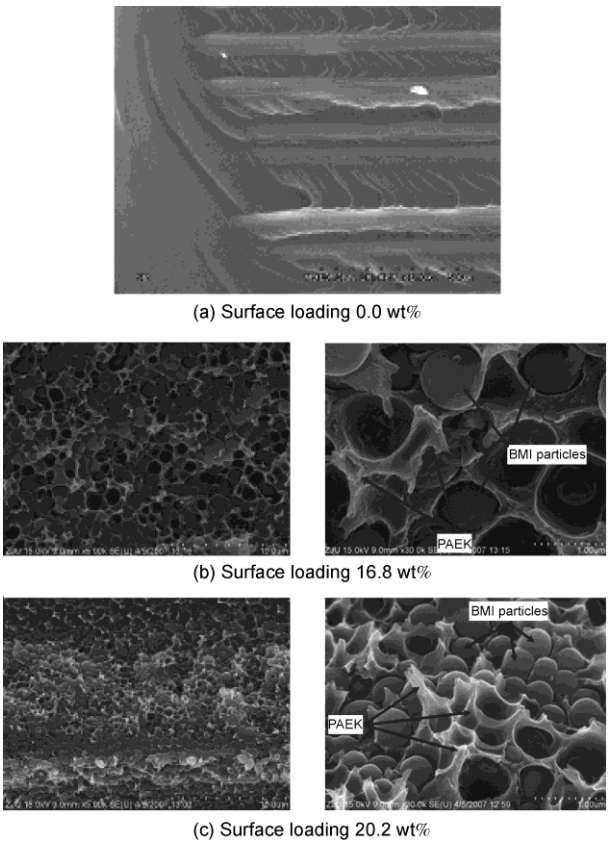

Figure 11 Representative SEM images on the onset of crack propagation of 6421 BMI specimen under Mode II test, in dependence on the surface-loading levels.

Table 6 Fracture toughness of 6421 BMI composite specimens in dependence on the surface-loading conditions

Surface-loading level (wt%)	G_{IC} (J/m^2)/C_v %	G_{IIC} (J/m^2)/C_v %
0.0	215 / 11.6	510 / 2.75
16.8	453 / 9.13	971 / 3.26
20.2	627 / 3.19	905 / 5.37

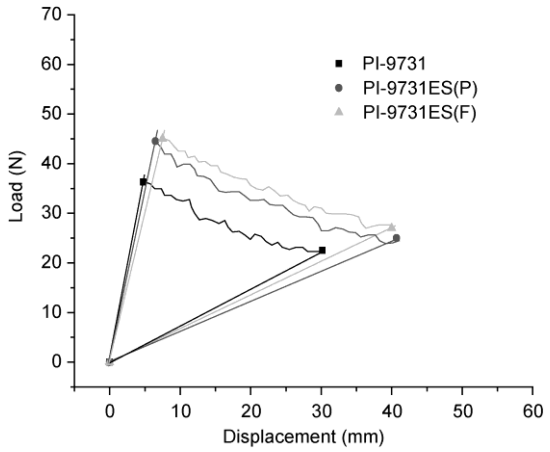

Figure 12 The load-displacement curves of the 9731 PI specimens in dependence on the surface-loading conditions.

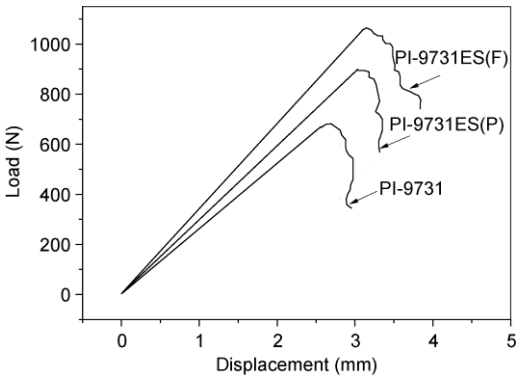

Figure 13 The load-displacement curves of the 9731 PI specimens in dependence on the surface-loading conditions.

Table 7 Fracture toughness of 9731 PI composite specimens in dependence on the surface-loading conditions

	Control (Untoughened)	Preform-based toughened	
		(P)	(F)
G_{IC}	310	410	459
G_{IIC}	590	939	1100

cteristic for 9731 PI composites preform-based toughened (Figures 14 and 15). The nodule size of the thermosetting polyimide was estimated approximately in the range of 30–50 nm (Figure 14(b)), resulting possibly again from the spinodal decomposition and inversion. It is not well understood why the microstructure should be so fine, but one possible explanation is the similar molecular structure of thermosetting 9731 with its thermoplastic toughener 9731T, making the two components compatible in a wide range. Under Mode I condition, the nodules were also plastically deformed (Figures 14(b) and 15(b)).

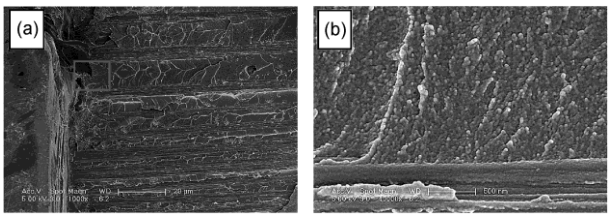

Figure 14 SEM images of fracture surface of 9731 PI composite toughened with 9731T (P) where (b) is a higher magnification of (a).

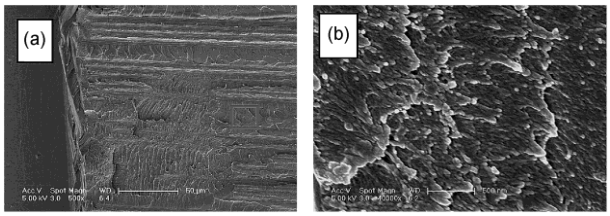

Figure 15 SEM images of fracture surface of 9731 PI composite toughened with 9731T (F) where (b) is a higher magnification of (a).

The aforementioned results clearly show that the liquid-molded BMI and PI high-temperature composite specimens can be made to have properties that are equivalent to the prepreg-based ones, even exceed those particularly the higher CAI target. By taking their particle and/or nodular microstructure into consideration, it is believed that the co-continuous microstructure is responsible for the improved impact damage resistance and fracture toughness performance. Especially, the remarkable plastic deformation of the brittle particles and/or nodules, embedded in respective thermoplastic phase, is rarely found anywhere else. The phenomenon leads to that there might be a hydrostatic condition that makes the plastic deformation possible. It is obvious that more intensive investigations are needed to understand the mechanism.

4 Conclusion

The use of carbon fiber fabrics surface-loaded with thermoplastic toughener has conclusively demonstrated the excellent toughening effect for high-temperature composites resin-transfer-molded. Moreover, the application of the preform-based toughening is compatible with the existing RTM technologies and adds very little labor cost to the production. Test data included herein show that it is possible to achieve the performance of the state-of-the-art prepreg material and that the in-plane mechanical properties are not compromised.

This work was supported by the National Basic Research Program of China ("973" Program) (Grant No. 2010CB631100).

1 Tsotsis T K. Interlayer toughening of composite materials. Polym Compos, 2008, DOI 10.1002/pc.20535
2 Yi X S, An X F, Tang B M, et al. *Ex-situ* formation of periodic interlayer structure to significantly improve the impact damage resistance of carbon laminates. Adv Eng Mater, 2002, 14(83): 3117–3122
3 An X F, Ji S Y, Tang B M, et al. Toughness improvement of carbon laminates by periodic interleaving thin thermoplastic films. J Mater Sci Lett, 2002, 21: 1763–1765
4 Long W, Xu J, Yi X S, et al. A preliminary study on resin transfer molding of highly toughed carbon laminates by *ex-situ* method. J Mater Sci Lett, 2003, 22: 1763–1765
5 Yi X S, An X F. Effect of interleaf sequence on impact damage and residual strength in a graphite/epoxy laminate. J Mater Sci Lett, 2004, 22: 3253–3255
6 Yi X S. Theory and Application of High-performance Polymer Matrix Composites (in Chinese). Beijing: National Defense Industry Press, 2011
7 Yi X S, An X F, Tang B M, et al. A Toughened Composite Laminate and a Process forPreparing the Same. PCT Patent No. FP1060809P, 2010.8.4
8 Yi X S, An X F, Zhang M, et al. A Preform for Liquid Molding Technology of Composites and the Process for Manufacturing Them. Chinese Patent No. ZL200510075276.7, 2010.9.8
9 Trademark Registration (in Chinese). No. 6962151, 6962152, 6962153. Beijing, 2010.5.28
10 Cheng Q F. Studies on Toughening Composites based on BMI Resin by *Ex-Situ* Concept (in Chinese). Disertation of Doctoral Degree. Hangzhou: Zhejiang University, 2007
11 Liu Z Z, Guo E, Xing J, et al. Application of carbon fiber/RTMable polyimide composites by *Ex-situ* toughening method. Acta Materiae Compositae Sinica, 2010, 27 (6): 1–8
12 Inoue T. Reaction-induced phase decomposition in polymer blends. Prog Polym Sci, 1995, 20: 119–153